frontiers | Frontiers in Plant Science

TYPE Original Research
PUBLISHED 26 August 2025
DOI 10.3389/fpls.2025.1455533

OPEN ACCESS

EDITED BY
Wilhelm Boland,
Max Planck Institute for Chemical Ecology, Germany

REVIEWED BY
Ferit Kocacinar,
Kahramanmaras Sütçü Imam University, Türkiye
Marko Kolaksazov,
Institute of Forage Crops, Bulgaria

*CORRESPONDENCE
Huajing Kang
kanghuajing@126.com

RECEIVED 27 June 2024
ACCEPTED 01 August 2025
PUBLISHED 26 August 2025

CITATION
Niu Z, Ye Z-W-Y, Huang Q, Peng C and Kang H (2025) Accuracy of photorespiration and mitochondrial respiration in the light fitted by CO_2 response model for photosynthesis. *Front. Plant Sci.* 16:1455533. doi: 10.3389/fpls.2025.1455533

Accuracy of photorespiration and mitochondrial respiration in the light fitted by CO_2 response model for photosynthesis

Zhengwen Niu[1], Zi-Wu-Yin Ye[2], Qi Huang[1], Chunju Peng[1] and Huajing Kang[1]*

[1]Wenzhou Key Laboratory of Agricultural & Forestry Carbon Sequestration and Tea Resource Development, Wenzhou Academy of Agricultural Sciences, Wenzhou, Zhejiang, China, [2]College of International Studies, Guangdong Baiyun University, Guangzhou, Guangdong, China

Introduction: Atmospheric CO_2 elevation significantly impacts plant carbon metabolism, yet accurate quantification of respiratory parameters—photorespiration rate (R_p) and mitochondrial respiration rate in the light (R_d)—under varying CO_2 remains challenging. Current CO_2-response models exhibit limitations in estimating these parameters, hindering predictions of crop responses under future climate scenarios.

Methods: Low-oxygen treatments and gas exchange measurements, calculating CO_2 recovery/inhibition ratio in of wheat (*Triticum aestivum L.*) and bean (*Glycine max L.*) were employed to elucidate the biological significance and interrelationships of R_p and R_d. Model-derived estimates of R_p and R_d were compared with measured values to assess the accuracy of three CO_2-response models (biochemical, rectangular hyperbola, modified rectangular hyperbola). Furthermore, the effects of ambient CO_2 concentration (0~1200 μmol·mol^{-1}) on the measured R_p and R_d were quantified through polynomial regression.

Results: The A/C_a model achieved superior fitting performance over the A/Ci model. However, significant disparities persisted between A/Ca-derived R_p/R_d estimates and measurements ($p < 0.05$). CO_2 concentration exhibited dose-dependent regulation of respiratory fluxes: $R_{p\text{-measured}}$ ranged from 4.923 ± 0.171 to 12.307 ± 1.033 μmol (CO_2) m^{-2} s^{-1} (wheat) and 4.686 ± 0.274 to 11.673 ± 2.054 μmol (CO_2) m^{-2} s^{-1} (bean), while $R_{d\text{-measured}}$ varied from 0.618 ± 0.131 to 3.021 ± 0.063 μmol (CO_2) m^{-2} s^{-1} (wheat) and 0.492 ± 0.069 to 2.323 ± 0.312 μmol (CO_2) m^{-2} s^{-1} (bean). Polynomial regression revealed strong non-linear correlations between CO_2 concentrations and respiratory parameters ($R^2 > 0.891$, $p < 0.05$; except bean R_p-C_a: $R^2 = 0.797$). Species-specific CO_2 thresholds governed peak R_p (600 μmol·mol^{-1} for wheat vs. 1,000 μmol·mol^{-1} for bean) and R_d (400 μmol·mol^{-1} for wheat vs. 200 μmol·mol^{-1} for bean).

Discussion: These findings expose critical limitations in current respiratory parameter quantification methods and challenge linear assumptions of CO_2-respiration relationships. They establish a critical framework for refining photosynthetic models by incorporating CO_2-responsive respiratory

mechanisms. The identified non-linear regulatory patterns and model limitations provide actionable insights for advancing carbon metabolism theory and optimizing crop carbon assimilation strategies under rising atmospheric CO_2, with implications for climate-resilient agricultural practices.

KEYWORDS

CO2 concentration, CO2 recovery, mitochondrial respiration rate, photorespiration, global change

1 Introduction

Atmospheric CO_2 concentration has increased by 48% since the pre-industrial era, reaching 415 ppm in 2021 (IPCC, 2021). This elevation drives dual climate-ecosystem impacts: as a primary greenhouse gas contributing to global warming through radiative forcing, and as a photosynthetic substrate enhancing plant productivity via the "CO_2 fertilization" effect (Easterling et al., 2000; Vaughan et al., 2003). However, the physiological mechanisms underlying plant adaptation to elevated CO_2—particularly regarding respiratory metabolism—remain insufficiently quantified (Xanthopoulos et al., 2017; Jalali et al., 2020).

Photosynthesis, transpiration, and respiration are three vital processes in plant life, essential for growth and metabolism (Nilsen, 1995). Transpiration facilitates water transport across the soil-plant-atmosphere continuum (SPAC), supporting plant growth and influencing ecosystem water-heat balances (Liu and Yu, 1997). Photosynthesis allows plants to convert light energy, CO_2, and water into organic matter and oxygen, directly impacting the productivity of terrestrial ecosystems and the global carbon cycle (Schimel et al., 2001). Photorespiration, however, occurs when the photosynthetic enzyme Rubisco reacts with oxygen instead of CO_2—a common scenario under high temperature, drought, or intense light that limits CO_2 availability. This process, universal in oxygen-producing plants and algae (Carvalho et al., 2011), shares chloroplasts as the primary site with photosynthesis and relies on light-driven reactions. Crucially, photorespiration recycles harmful byproducts generated during photosynthesis, balancing energy use and protecting plants from stress, thereby acting as a "safety valve" for photosynthetic efficiency. Mitochondrial respiration involves oxidative phosphorylation in the cells' mitochondria to produce energy for vital activities (Vercellino and Sazanov, 2022; Huang et al., 2023). These biological processes adapt to elevated CO_2 concentrations and climate warming (Luo et al., 2001), affecting carbon cycling processes in terrestrial ecosystems (Lin, 1998; Zhang et al., 2000; Wang et al., 2008). Thus, understanding how crop photorespiration and mitochondrial respiration respond to changes in atmospheric CO_2 is crucial for predicting future crop productivity and growth patterns under elevated CO_2 conditions.

Wheat and bean are globally significant crops, crucial to human food supply and agricultural production (Gan et al., 2015; Borrell et al., 2017). As typical C_3 plants, CO_2 is the main limiting factor affecting their photosynthesis (Atkin et al., 2005). Traditional theories suggest that the carbon source for photosynthesis in terrestrial plants is primarily atmospheric CO_2, often neglecting CO_2 released by photorespiration and dark respiration of the leaves (Stirbet et al., 2020). And related respiration parameters (photorespiration rate (R_P), mitochondrial respiration rate in the light (R_d), and respiration in the light (R_L)) are inconsistently applied (von Caemmerer, 2000). The chloroplast interior constitutes the primary site for photorespiratory CO_2 release, where a substantial proportion of respired CO_2 undergoes re-assimilation through the Calvin cycle. This CO_2 recycling mechanism plays a crucial physiological role by enhancing subcellular CO_2 concentration independent of diffusion limitations imposed by boundary layer resistance stomatal conductance, and mesophyll resistance (Loreto et al., 1999, 2001; Pinelli and Loreto, 2003). Quantitatively studying photorespiratory CO_2 recycling in C_3 plants is challenging due to the simultaneous occurrence of photorespiration, dark respiration, and photosynthetic carbon assimilation within mesophyll cells (Haupt-Herting et al., 2001). The carbon isotope method can distinguish between CO_2 fixed by photosynthesis and released by photorespiration, offering a potential approach to studying CO_2 recycling and reuse by plants (Ostle et al., 2000). However, this method is costly, complex, and not precise in exploring photorespiratory CO_2 recycling, because this method ignores two important factors: firstly, Rubisco's affinity for $^{14}CO_2$ and $^{13}CO_2$ is much lower than that of $^{12}CO_2$; secondly, the measurement process inevitably involves the inhibition of photorespiration by extremely high concentrations of $^{12}CO_2$ (30000 μmol mol^{-1}) (Pärnik and Keerberg, 2007; Busch and Sage, 2017). Kang et al. (2014) used gas exchange methods to confirm that CO_2 released by light and dark respiration can be reutilized by photosynthesis, though this concept is often overlooked. Therefore, accurate estimation of photorespiratory CO_2 reutilization is essential for improving the accuracy of photosynthetic parameters and carbon metabolism processes.

The CO_2 response curve for photosynthesis is a valuable tool for studying plant physiology and ecology, providing insights into how photosynthetic properties respond to environmental factors. This understanding can optimize CO_2 concentration management in agricultural production, contributing to enhance photosynthetic efficiency and promote growth and productivity. Two types of

CO_2 response models exist: biochemical and empirical. The most widely used biochemical model is the Farquhar model and its modifications (von Caemmerer and Farquhar, 1981; Bernacchi et al., 2001; Long and Bernacchi, 2003; Ethier and Livingston, 2004). Empirical models include the rectangular hyperbola model (Ye, 2010), modified version (Ye and Yu, 2009), and the Michaelis-Menten model (Harley et al., 1992). However, current biochemical models do not consider the effect of mitochondrial respiration rate in the light (R_d), and empirical models overlook the effect of CO_2 concentration on photorespiration rate. Quantitative studies on the effect of atmospheric CO_2 concentration (C_a) on R_p and R_d are limited, making the accuracy of R_p and R_d values from current CO_2 response models uncertain.

Addressing these research gaps, this study used low oxygen and gas exchange methods, with calculating CO_2 recovery and inhibition ratio, aiming to: (1) elucidate the biological significance and interrelationships of photosynthetic parameters related to light and dark respiration, and accurately measure or calculate them; (2) compare R_p and R_d values between fitted and measured data to evaluate the CO_2 photosynthetic response model's accuracy, identifying a more precise estimation model (A/C_a or A/C_i); and (3) provide quantitative descriptions of C_a or C_i (depends on the accuracy of the model) effects on $R_{p\text{-measured}}$ and $R_{d\text{-measured}}$, offering theoretical research insights for the practical application of photosynthetic carbon metabolism processes and the promotion of carbon metabolism.

2 Materials and methods

2.1 CO_2 response models

The biochemical model can be expressed as

$$P_n = min\{w_c\ ,\ w_j\ ,\ w_p\}\left(1-\frac{\tau^*}{C_i}\right)-R_d \quad (1)$$

where P_n is the net photosynthetic rate; and w_c, w_j and w_p are the potential rates of CO_2 assimilation that can be supported by the enzymes of ribulose 1,5-bisphosphate (RuBP) carboxylase/oxygenase (Rubisco), RuBP- regeneration and triose-phosphate utilization, respectively. The photosynthetic compensation point (τ^*) is the CO_2 concentration at which the photorespiratory efflux of CO_2 equals the rate of photosynthetic CO_2 uptake. C_i is the intercellular CO_2 concentration and R_d is the mitochondrial respiration rate in the light.

Empirical models include the rectangular hyperbola model, modified version, and the Michaelis-Menten model, as following:

The rectangular hyperbola model can be represented as

$$P_n = \frac{aP_{nmax}C_i}{aC_i + P_{nmax}} - R_p \quad (2)$$

where P_{nmax} is the maximum photosynthetic rate; R_p is the photorespiration rate (in fact this parameter represents the respiration rate in the light (R_L), which includes R_p and R_d. A detailed description is given in the text.); and α is the initial slope of the CO_2 response curve; C_i is the same as above.

The Michaelis–Menten model can be displayed as

$$P_n = \frac{P_{nmax}C_i}{C_i + K} - R_p \quad (3)$$

where P_{nmax}, R_p, P_n and C_i are the same as above, and K is the Michaelis-Menten constant.

The modified rectangular hyperbola model can be written as

$$P_n = a\frac{1-bC_i}{1+cC_i}C_i - R_p \quad (4)$$

where α, R_p, P_n and C_i are the same as above, and b and c are coefficients (mol μmol^{-1}) (Ye, 2010) (Equations 1–4).

According to this equation, the Michaelis-Menten and the rectangular hyperbola model are essentially the same. Therefore, the fitted results for the Michaelis-Menten model were not shown in this paper.

2.2 Theoretical considerations

2.2.1 Calculation of photorespiration rates

R_p were determined through differential gas exchange measurements under contrasting O_2 concentrations. Measurements were conducted using a LI-6400XT portable photosynthesis system (LI-COR Biosciences, Lincoln, NE, USA) with the following standardized conditions:

1. Ambient O_2 treatment (21% O_2): At ambient CO_2 (0 $\mu mol \cdot mol^{-1}$) and saturating Photosynthetically Active Radiation (PAR) (2000 $\mu mol \cdot m^{-2} \cdot s^{-1}$), the net photosynthetic rate ($P_{n21\%}$) represents combined respiratory fluxes ($R_L = R_p + R_d$), as photorespiration proceeds normally while CO_2 in photosynthesis comes from respiration.
2. Low O_2 treatment (2% O_2): Under identical CO_2 and light conditions, complete inhibition of photorespiration in wheat and bean leaves was achieved based on our previous validation (Kang et al., 2014). The measured $P_{n2\%}$ thus corresponds specifically to R_d.

R_p was calculated using the respiratory partitioning equation (Erdei et al., 2001; Laisk et al., 2002; Parys et al., 2004):

$$R_p = P_{n2\%} - P_{n21\%} \quad (5)$$

where $P_{n2\%}$ and $P_{n21\%}$ are the photosynthetic rates at 2% O_2 and 21% O_2, respectively.

2.2.2 Calculation of CO_2 recovery and inhibition ratios of photorespiration

Our prior mechanistic studies revealed concentration-dependent regulation of photorespiratory CO_2 recovery. The photorespiratory CO_2 recovery ratio ($R_{pe\text{-}i}$), defined as the

proportion of respired CO_2 re-assimilated by chloroplasts, decreased progressively with increasing ambient CO_2 concentration. Beyond threshold CO_2 concentrations, competitive inhibition between photorespiration and carboxylation pathways significantly suppressed photorespiratory flux (Kang et al., 2013). $R_{pe\text{-}i}$ and photorespiratory inhibition index (I_i) can be quantified through Equation 6.

$$R_{pe-i} \quad or \quad I_i = \frac{R_{pmax} - R_{p-i}}{R_{pmax}} \tag{6}$$

where R_{pe-i} and I_i are the CO_2 recovery ratio and inhibition ratio of photorespiration, $R_{p\max}$ is the maximum photorespiration rate and R_{p-i} is the photorespiration rate at i CO_2 concentrations, i represents different CO_2 concentrations.

2.2.3 Calculation of the mitochondrial respiration rates in the light

Both mitochondrial respiration-derived CO_2 and photorespiration-derived CO_2 originate from the same cellular compartment, i.e., mitochondria. Given this shared origin, it follows that CO_2 released through mitochondrial respiration undergoes similar refixation dynamics as photorespiratory CO_2 under low atmospheric CO_2 concentrations (C_a) and is comparably inhibited at elevated C_a. The recovery efficiency and inhibition ratio of mitochondrial respiration-derived CO_2 were consequently equivalent to those observed in photorespiration. To quantify R_d, we therefore integrated the maximum mitochondrial respiration rate (R_n) with the photorespiration-associated parameters $R_{pe\text{-}i}$ and I_i, using the following calculation scheme:

$$R_{d-i} = R_{n-i} \times (1 - R_{pe-i}) \quad or \quad R_{d-i} = R_{n-i} \times (1 - I_i) \tag{7}$$

where R_{d-i} and R_{n-i} represent mitochondrial respiration rates under light and dark conditions, respectively, at a given atmospheric CO_2 concentration.

2.2 Study site and plants

The experiment was conducted at the Yucheng Comprehensive Experiment Station (36°50′N, 116°34′E; 20.3 m elevation) of the Chinese Academy of Sciences, located in the lower Yellow River basin. This semi-arid region exhibits a mean annual temperature of 13.4°C and receives 567 mm of precipitation annually, with 70% occurring between June and September (1985–2009 climate normals). The soil is classified as calcaric fluvisol (FAO-UNESCO system) with silt loam texture (12% sand, 66% silt, 22% clay; USDA classification) and pH 8.6 (Hou et al., 2012).

Wheat and bean were sown on 4 October 2013 and 3 May 2014, respectively. Field-grown plants experienced maximum photosynthetic photon flux density (PPFD) of 2000 μmol m^{-2} s^{-1} during sunny days. Measurements were conducted during key phenological stages: wheat from 12 ~ 25 May (characterized by 7 sunny days, predominantly cloudy skies, no effective precipitation, and a mean temperature of 29°C) and bean from 16 ~ 25 June (marked by predominantly cloudy conditions, 95 mm rainfall, and an average temperature of 30°C) 2014. We randomly sampled vigorous plants with homogeneous growth and measured the apical leaf of the fifth compound leaf (numbered from the base upward) on each seedling.

2.3 CO_2 gas exchange measurement

Leaf-level CO_2 exchange was quantified using a LI-6400XT portable photosynthesis system (LI-COR Biosciences, Lincoln, NE, USA) during two daily intervals (09:00 ~ 11:30 and 14:30 ~ 17:00). For each species, the leaves were acclimated in the cuvette for 15 min to stabilize gas exchange prior to measurements. Environmental conditions were maintained at leaf temperature 30 ± 0.3°C (wheat) or 33 ± 1.7°C (bean) with 60% relative humidity. Two sets of CO_2 response curves were generated by systematically exposing leaves to a sequence of 12 atmospheric CO_2 concentrations (C_a: 0, 50, 80, 100, 150, 200, 380, 400, 600, 800, 1,000, and 1,200 μmol mol^{-1}). These experiments were conducted under two distinct oxygen conditions: ambient (21% O_2) and low-oxygen (2% O_2). For measurements of R_p, R_d, and other related parameters, a PAR of 2000 μmol m^{-2} s^{-1} was used. Conversely, a PAR of 0 μmol m^{-2} s^{-1} was employed to determine the mitochondrial respiration rates in the dark (Kang et al., 2014). The hypoxic gas mixture (2% O_2) was supplied by Xinjian Air Plant (Yucheng, Shandong) and humidified via a 1.2 m^3 buffer bag containing distilled water prior to entering the gas analyzer.

2.4 Statistics

Photosynthetic parameters were derived using Photosynthesis Assistant software (LI-COR Biosciences). Non-linear regression analyses implemented in SPSS 11.5 (IBM Corp., Armonk, NY, USA), based on Levenberg-Marquardt algorithm, including rectangular hyperbola model and Standard rectangular hyperbola model.

Treatment effects were assessed by two-way ANOVA with Tukey's *post-hoc* test, while pairwise comparisons employed two-tailed Student's t-tests ($p< 0.05$). All statistical visualizations were generated using GraphPad Prism 4.0c (GraphPad Software, San Diego, CA).

3 Results

3.1 Respiratory flux partitioning

At saturating irradiance (2000 μmol photons m^{-2} s^{-1}), mitochondrial respiration ($R_{L\text{-measured}}$) reached 6.548 ± 0.136 and 6.334 ± 0.342 μmol (CO_2) m^{-2} s^{-1} in wheat and bean, respectively. $R_{d\text{-measured}}$ exhibited the values of 2.036 ± 0.276 (wheat) and 1.893 ± 0.075 μmol (CO_2) m^{-2} s^{-1} (bean). $R_{p\text{-measured}}$ calculated via Equation 5 at zero CO_2 ($R_{p\text{-}0\text{-measured}}$) showed interspecific divergence, with wheat (4.511 ± 0.412 μmol (CO_2) m^{-2} s^{-1}) and

10.3389/fpls.2025.1455533

TABLE 1 Compared between measured and fitted values of R_L, R_d, and R_{p-0} for wheat and bean.

Measured		Wheat		Bean	
$R_{L\text{-}measured}$ (21% O_2)		6.548 ± 0.136 a		6.334 ± 0.342 a	
$R_{d\text{-}measured}$ (2% O_2)		2.036 ± 0.276 c		1.893 ± 0.075 c	
$R_{p\text{-}0\text{-}measured}$		4.511 ± 0.412 b		4.686 ± 0.274 b	
Fitted Models		$R_{L\text{-}fitted}$ (21% O_2)		$R_{d\text{-}fitted}$ (2% O_2)	
		Wheat	Bean	Wheat	Bean
A/C_i	Biochemical model	21.067 ± 0.115*	17.600 ± 0.970*	6.333 ± 0.611#	4.700 ± 0.476#
	Rectangular hyperbola model	17.108 ± 0.978*	14.380 ± 0.680*	7.757 ± 1.155#	5.849 ± 1.283#
	Modified rectangular hyperbola models	14.172 ± 0.156*	12.713 ± 0.319*	5.599 ± 0.521#	4.612 ± 0.517#
A/C_a	Biochemical model	20.667 ± 0.577*	6.850 ± 0.379*	20.200 ± 1.114#	2.467 ± 0.231#
	Rectangular hyperbola model	8.428 ± 1.100*	7.510 ± 0.545*	4.059 ± 1.277#	3.837 ± 0.493#
	Modified rectangular hyperbola models	7.353 ± 0.455*	7.102 ± 0.523*	2.716 ± 0.493#	2.779 ± 0.437#

The data represent the mean ± SD of five independent experiments; Measured values of R_L, R_p and R_d for wheat and bean at 2000 μmol m^{-2} s^{-1} when the CO_2 concentration was 0 μmol mol^{-1}; Different letters at the same species indicate significant differences at the $P< 0.05$ level; * indicates that there are significant differences at the $P< 0.05$ level between the fitted values for $R_{L\text{-}fitted}$ and the measured values of $R_{L\text{-}measured}$ (21% O_2). # indicates that there are significant differences of $R_{d\text{-}measured}$ at the $P< 0.05$ level between the fitted values and the measured values (2% O_2).

bean (4.686 ± 0.274 μmol (CO_2) m^{-2} s^{-1}), we can find that there were significantly different between $R_{L\text{-}measured}$ and $R_{p\text{-}measured}$ (Table 1).

3.2 Model performance evaluation

The three CO_2 response models (biochemical, rectangular hyperbola, modified rectangular hyperbola) were evaluated by comparing $R_{L\text{-}fitted}$ (21% O_2) and $R_{d\text{-}fitted}$ (2% O_2) values with experimental measurements (Table 1).

Under the A/C_i framework, the modified rectangular hyperbola model showed the smallest deviations for both $R_{L\text{-}fitted}$ and $R_{d\text{-}fitted}$ compared to biochemical and rectangular hyperbola models. For example, $R_{L\text{-}fitted}$ in wheat were 14.172 ± 0.156 μmol m^{-2} s^{-1} (modified model) versus 21.067 ± 0.115 (biochemical) and 17.108 ± 0.978 (rectangular), contrasting with measured values of 6.548 ± 0.136 ($P< 0.05$ for biochemical and rectangular models). Similar trends were observed for $R_{d\text{-}fitted}$ (Table 1). Under the A/C_a framework, the modified model exhibited further accuracy improvements, particularly for $R_{d\text{-}fitted}$. For wheat, A/C_a-based $R_{d\text{-}fitted}$ estimates (2.716 ± 0.493 μmol m^{-2} s^{-1}) reduced deviations from measured values by 80.915% compared to A/C_i predictions (5.599 ± 0.521; Δ = 3.563 vs. 0.680 μmol m^{-2} s^{-1}). In bean, A/C_a $R_{d\text{-}fitted}$ errors decreased by 67.414% (Δ = 2.719 vs. 0.886 μmol m^{-2} s^{-1}). $R_{L\text{-}fitted}$ estimations under A/C_a also approached measured values more closely than under A/C_i.

The modified rectangular hyperbola model under A/C_a framework demonstrated optimal consistency with experimental data, justifying its selection for subsequent analyses of respiratory responses to ambient CO_2 (C_a).

3.3 Photorespiration rate ($R_{p\text{-}measured}$) responses to C_a

$R_{p\text{-}measured}$ exhibited a unimodal relationship with ambient CO_2 concentration in both wheat and bean, characterized by an initial increase followed by a decline at elevated C_a levels. The $R_{p\text{-}measured}$ values ranged from 4.923 ± 0.171 to 12.307 ± 1.033 μmol (CO_2) m^{-2} s^{-1} for wheat (Figure 1A) and 4.686 ± 0.274 to 11.673 ± 2.054 μmol (CO_2) m^{-2} s^{-1} for bean (Figure 1B), with polynomial regression models demonstrating strong correlations (R^2 = 0.923 for wheat, R^2 = 0.797 for bean).

Crop-specific differences were evident in the C_a thresholds corresponding to peak $R_{p\text{-}measured}$. Wheat achieved maximum $R_{p\text{-}measured}$ (12.307 ± 1.033 μmol (CO_2) m^{-2} s^{-1}) at 600 μmol mol^{-1} C_a, whereas bean exhibited peak $R_{p\text{-}measured}$ (11.673 ± 2.054 μmol (CO_2) m^{-2} s^{-1}) at 1000 μmol mol^{-1} C_a (Figures 1A, B).

3.4 Mitochondrial respiration rate in the light ($R_{d\text{-}measured}$) responses to C_a

$R_{d\text{-}measured}$, derived from Equation 7, exhibited a unimodal relationship with C_a for both species. The $R_{d\text{-}measured}$ values ranged from 0.618 ± 0.131 to 3.021 ± 0.063 μmol (CO_2) m^{-2} s^{-1} for wheat (Figure 2A) and 0.492 ± 0.069 to 2.323 ± 0.312 μmol (CO_2) m^{-2} s^{-1} for bean (Figure 2B), with polynomial regression models demonstrating strong correlations (R^2 = 891 for wheat, R^2 = 0.892 for bean). $R_{d\text{-}measured}$ initially increased to peak values of 3.021 ± 0.063 μmol (CO_2) m^{-2} s^{-1} (wheat) and 2.323 ± 0.312 μmol (CO_2) m^{-2} s^{-1} (bean), followed by declines at elevated C_a. Polynomial

10.3389/fpls.2025.1455533

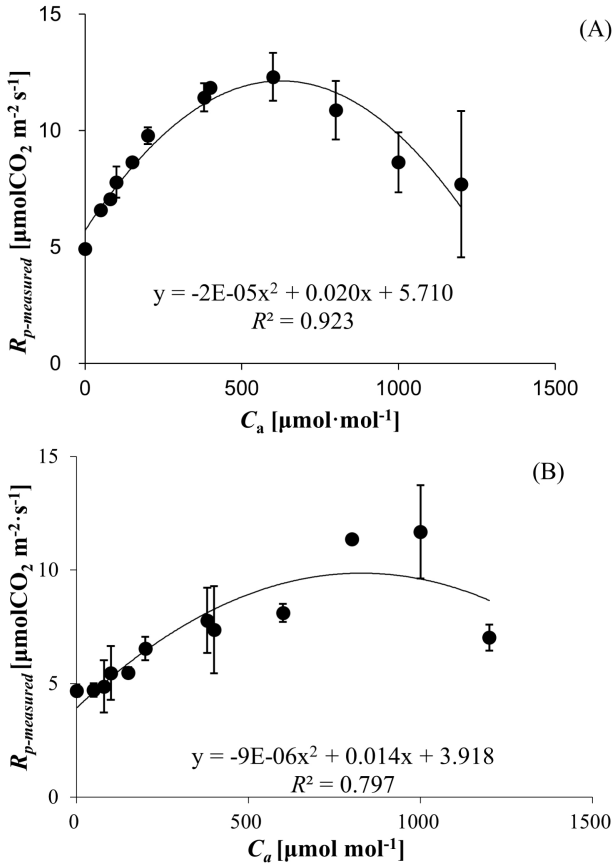

FIGURE 1
(A) Photorespiration rates (*Rp-measured*) of wheat responses to C_a. **(B)** Photorespiration rates (*Rp-measured*) of bean responses to C_a.

regression confirmed robust correlations, reflecting C_a-dependent modulation of $R_{d\text{-measured}}$ dynamics.

3.5 Mitochondrial respiration in the dark ($R_{n\text{-measured}}$) responses to C_a and O_2 concentration

$R_{n\text{-measured}}$ declined progressively with increasing C_a for both wheat and bean, independent of O_2 levels (21% vs. 2%). At 21% O_2, R_n spanned 1.453 ± 0.603 to 3.862 ± 0.557 μmol (CO_2) m^{-2} s^{-1} (wheat, Figure 3A) and 1.210 ± 0.340 to 4.040 ± 0.167 μmol (CO_2) m^{-2} s^{-1} (bean, Figure 3B). Under 2% O_2, the ranges shifted to 1.512 ± 0.674 to 4.101 ± 0.297 (wheat) and 0.817 ± 0.607 to 3.718 ± 0.519 μmol (CO_2) m^{-2} s^{-1} (bean). Strong negative correlations between R_n and C_a were observed (R^2 = 0.969 for wheat, R^2 = 0.977 for bean), with no significant O_2 concentration effect ($P > 0.05$).

3.6 Recovery (R_{pe-i}) and inhibition (I_i) ratios response to C_a

As mentioned before, 12.307 ± 1.033 and 11.673 ± 2.054 μmol (CO_2) m^{-2} s^{-1} were the maximum photorespiration rate values for wheat and bean, respectively. On this basis, the CO_2 recovery and inhibition ratios for photorespiration at different CO_2 concentrations were estimated according to Equation 6. As C_a increased, the recovery ratios decreased from 59.995% (wheat) and 66.869% (bean) to zero, respectively (Figure 4). After that, the inhibition ratios increased sharply, reaching 57.456% (wheat) and 39.845% (bean), respectively.

4 Discussion

4.1 Respiratory flux partitioning

In the framework of traditional models, the overall respiration rate under light conditions (R_L), which aggregates the rates of photorespiration (R_p) and mitochondrial respiration in the light (R_d), has frequently been either conflated with photorespiration alone (Zelitch, 1980; Ye and Yu, 2009; von Caemmerer, 2000) or has overlooked the significance of the reutilization of CO_2 released during photorespiration (Kang et al., 2014). This conflation or oversight tends to result in a marked discrepancy between the observed photorespiration rates ($R_{p\text{-fitted}}$) and their actual values. Our empirical findings, obtained under conditions of 21% O_2 and atmospheric CO_2 concentration of 0 μmol mol^{-1}, indicated that the

10.3389/fpls.2025.1455533

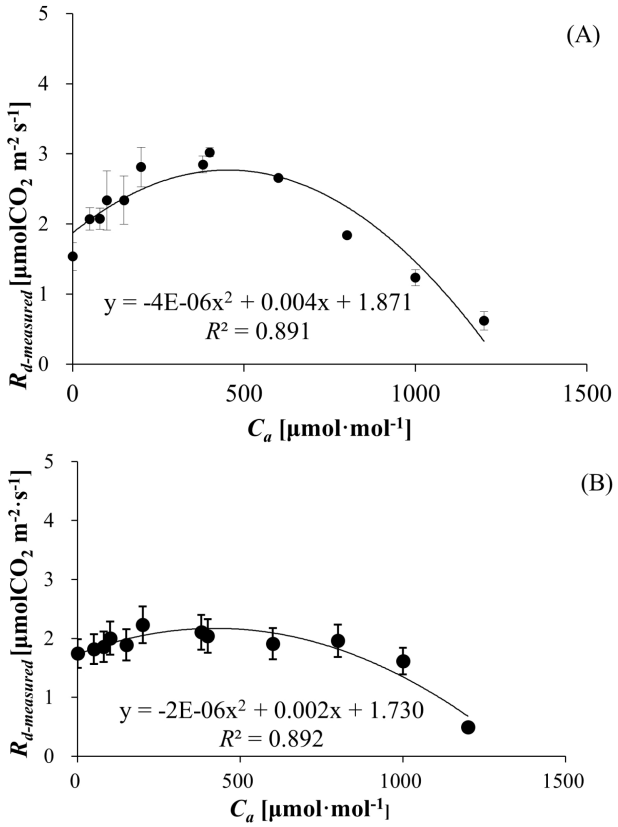

FIGURE 2
(A) Mitochondrial respiration rate in the light ($R_{n\text{-}measured}$) of wheat responses to C_a. **(B)** Mitochondrial respiration rate in the light ($R_{d\text{-}measured}$) of bean responses to C_a.

$R_{L\text{-}measured}$ values for wheat and bean (6.548 ± 0.136 and 6.334 ± 0.342 μmol m^{-2} s^{-1}, respectively) significantly surpassed the accurately determined photorespiration rates ($R_{p\text{-}0\text{-}measured}$ = 4.511 ± 0.412 and 4.686 ± 0.274 μmol m^{-2} s^{-1} for wheat and bean, respectively), as derived through the differential method ($R_{L\text{-}measured}$ − $R_{d\text{-}measured}$). This discrepancy underscores the systematic bias inherent in the traditional approach, which solely attributes R_L to photorespiration, thereby neglecting the distinct and crucial contribution of mitochondrial respiration under light conditions (R_d).

Our analysis sheds light on the intricate dynamics between photorespiration and mitochondrial respiration within the context of photosynthesis, challenging the conventional understanding that has, until now, inadequately accounted for the nuanced contributions of these two processes. By distinguishing between R_L and its constituent components, R_p and R_d, our study provides a more nuanced understanding of plant respiratory processes in the light, highlighting the significant role of R_d. This clarification is pivotal for refining existing photosynthetic models, ensuring a more accurate representation of plant respiratory mechanisms and their implications for carbon metabolism.

4.2 Model performance evaluation

In the realm of plant physiology, accurately modeling the intricate processes of photorespiration and mitochondrial respiration under photosynthetic conditions is pivotal. Our study, by comparing measured values with the fitted values (Table 1), underscores the remarkable precision of the Modified rectangular hyperbola models, especially when employing A/C_a curves for estimating $R_{L\text{-}fitted}$ and $R_{d\text{-}fitted}$ values. This finding aligns with the observations made by Ye and Yu (2009), who posited that the discrepancies observed in earlier models could be attributed to the misrepresentation of intercellular CO_2 concentrations by the C_i values used in those models.

However, a notable divergence persists between the fitted values generated by the A/C_a model and the actual measurements. This discrepancy led to the conclusion that previous models might have overlooked the significant impact of CO_2 concentration on R_d and R_p. Our analysis suggests an imperative need for further research aimed at refining these models to enhance their accuracy.

10.3389/fpls.2025.1455533

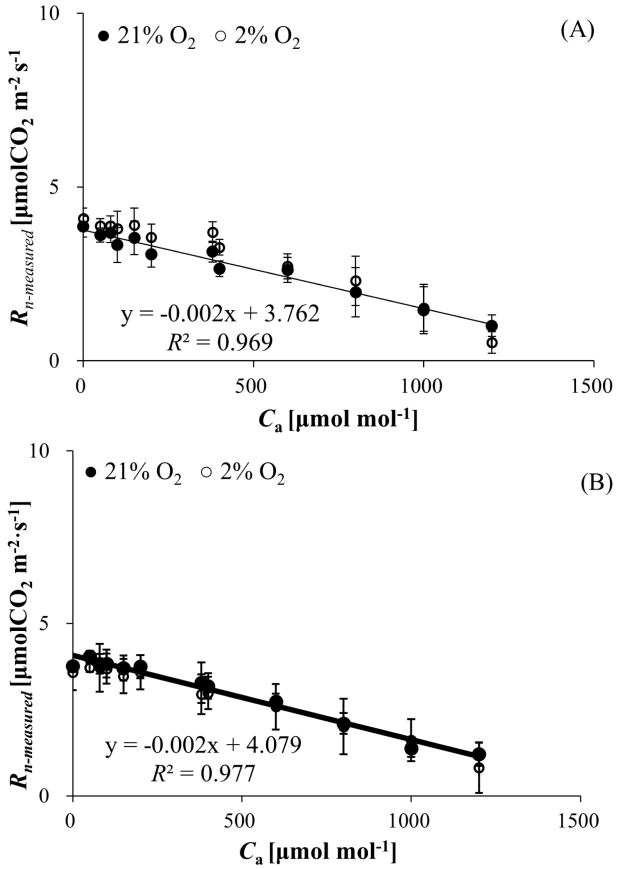

FIGURE 3
(A) Mitochondrial respiration rate in the dark ($R_{n\text{-}measured}$) of wheat responses to C_a and O_2 concentration. **(B)** Mitochondrial respiration rate in the dark ($R_{n\text{-}measured}$) of bean responses to C_a and O_2 concentration.

4.3 Photorespiration rate and Mitochondrial respiration rate in the light responses to C_a

This study revealed a nonlinear regulatory mechanism of CO_2 concentration on photorespiration rate ($R_{p\text{-}measured}$) and mitochondrial respiration rate in the light ($R_{d\text{-}measured}$) in C_3 plants: $R_{p\text{-}measured}$ increased with rising CO_2 concentrations when external CO_2 levels were below species-specific thresholds (600 μmol mol^{-1} for wheat and 1000 μmol mol^{-1} for bean), whereas exceeding these thresholds triggered a significant suppression of $R_{p\text{-}measured}$. As for $R_{d\text{-}measured}$, the thresholds were 400 μmol mol^{-1} for wheat and 200 μmol mol^{-1} for bean. This phenomenon can be explained by the dynamic interplay between RuBisCO enzyme activity and chloroplast microenvironmental conditions. At low CO_2 concentrations, although the carboxylation activity of RuBisCO is globally constrained by substrate limitation (Caemmerer and Edmondson, 1986) and RuBP regeneration becomes impaired (Badger et al., 1984), the CO_2 released during photorespiration is efficiently re-assimilated by photosynthesis due to its proximity to the chloroplast inner membrane (Yadav et al., 2020). This tight coupling between photorespiratory CO_2 release and photosynthetic refixation (Häusler et al., 2002; Loreto et al., 1999; Busch et al., 2013; Kang et al., 2013) partially mitigates the inhibitory effects of low CO_2 on the Calvin cycle. Concurrently, enhanced photosynthesis elevates chloroplast O_2 levels (Sharkey, 1988), temporarily promoting RuBisCO oxygenation activity and driving the "paradoxical" increase in R_p and R_d. However, when CO_2 concentrations surpass species-specific thresholds, the chloroplast CO_2/O_2 ratio undergoes a fundamental reversal (Brooks and Farquhar, 1985), favoring RuBisCO carboxylation through competitive substrate inhibition of oxygenation, leading to a decrease in $R_{p\text{-}measured}$ and $R_{d\text{-}measured}$. The observed threshold divergence between wheat and bean likely arises from two interconnected mechanisms: First, interspecific variations in RuBisCO kinetics (e.g., CO_2 affinity) and leaf anatomical adaptations regulating CO_2 diffusion resistance, consistent with the multiscale regulatory complexity of photorespiratory metabolism (Wang et al., 2020; Celebi-Ergin, 2022). Second, differential cellular metabolic demands—for example, the approximately twofold higher CO_2 threshold for peak photorespiration in bean (1,000 vs. 600 μmol·mol^{-1} in wheat) aligns with the hypothesis proposed by Krmer et al. (2022) that elevated photorespiratory flux in legumes supports nitrogen assimilation-coupled amino acid synthesis. These findings not only provided theoretical support for crop-specific CO_2

10.3389/fpls.2025.1455533

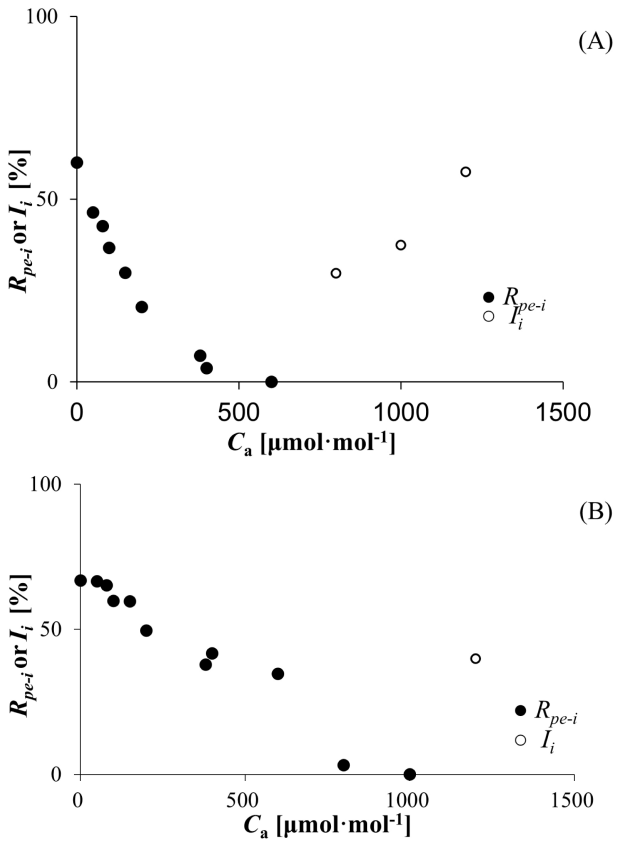

FIGURE 4
(A) Recovery and inhibition rates ($R_{pe\text{-}i}$ and I_i) of wheat responses to C_a. **(B)** Recovery and inhibition rates ($R_{pe\text{-}i}$ and I_i) of bean responses to C_a.

fertilization strategies in controlled-environment agriculture but also advance our understanding of carbon-oxygen metabolic homeostasis in C_3 plants.

4.4 Mitochondrial respiration rate in dark ($R_{n\text{-measured}}$) responses to C_a and O_2 concentration

Accurately estimating the dark respiration rate of a plant facilitates the calculation of its maximum carboxylation rate, respiration rate in the light, electron flow partitioning, and other important photosynthetic parameters (Wang et al., 2001; Yin et al., 2011). Oxygen is essential for the respiration process in plant cells (Moseley et al., 2018). However, the results of our experiments showed that there was no significant difference in dark mitochondrial respiration rates between wheat and bean at 2% and 21% O_2 (Table 1). It's meant to be sufficient oxygen for mitochondrial respiration at 2% O_2. In addition, we can notice that there is linear regulatory mechanism of CO_2 concentration on $R_{n\text{-measured}}$, i.e., the R_n decreased as C_a increased (Figures 3A, B), which was different from the relationship between $R_{d\text{-measured}}$, $R_{p\text{-measured}}$, and carbon dioxide. We speculate that this may be due to the increase in CO_2 concentration inhibiting the activity of certain enzymes related to dark respiration, and this effect is stronger than that of $R_{d\text{-measured}}$ and $R_{p\text{-measured}}$. Reuveni and Gale (1985) also obtained the similar results that CO_2 concentration has a strong effect on dark respiration rates in plants.

5 Conclusion

This study advanced our understanding of respiratory parameter estimation in C_3 plants by systematically evaluating the accuracy of photorespiration (R_p) and mitochondrial respiration in the light (R_d) derived from CO_2-response models. Key findings revealed that the modified rectangular hyperbola model under the A/C_a framework outperformed traditional A/C_i models in estimating R_p and R_d, yet significant discrepancies persisted between modeled and empirical values ($p< 0.01$), highlighting inherent limitations in current methodologies. Notably, CO_2 concentration exhibited dose-dependent, non-linear regulation of respiratory parameters. $R_{p\text{-measured}}$ in wheat and bean demonstrated unimodal responses to C_a, peaking at 600 and 1,000 μmol·mol^{-1}, respectively, before declining due to competitive inhibition of RuBisCO oxygenation. Similarly, $R_{d\text{-measured}}$ displayed different thresholds between bean and wheat (400 μmol mol^{-1} for wheat and 200 μmol mol^{-1} for bean.). The identification of strong polynomial correlations ($R^2 > 0.89$) between C_a and respiratory fluxes challenges conventional assumptions of linear responses,

emphasizing the need to integrate CO_2-responsive regulatory dynamics into photosynthetic models. Furthermore, dark respiration ($R_{n\text{-measured}}$) exhibited a linear decline with rising C_a, independent of O_2 concentration, suggesting distinct mechanistic controls compared to light-dependent respiration.

These findings provide critical insights for refining photosynthetic models by incorporating CO_2-mediated respiratory adjustments. The empirical relationships established here offer a framework for optimizing carbon assimilation strategies in crops under rising atmospheric CO_2, particularly in controlled-environment agriculture.

Data availability statement

The datasets presented in this article are not readily available because data privacy. Requests to access the datasets should be directed to kanghuajing@126.com.

Author contributions

HK: Conceptualization, Funding acquisition, Methodology, Supervision, Writing – review & editing. ZN: Investigation, Writing – original draft, Writing – review & editing. ZY: Data curation, Formal Analysis, Writing – review & editing. QH: Formal Analysis, Investigation, Writing – review & editing. CP: Investigation, Writing – review & editing.

Funding

The author(s) declare financial support was received for the research and/or publication of this article. This work was supported by the 863 Project under contract No. 2013AA102903, the National Key Technologies R & D Program of China No.2013BAD05B03, the Natural Science Foundation of China No. 31560069 and the Key Science and Technology Innovation Team Project of Wenzhou City No. C20150008.These funds provide expenses for data collection, measurement, and paper layout fees for this study.

Conflict of interest

The authors declare that the research was conducted in the absence of any commercial or financial relationships that could be constructed as a potential conflict of interest.

Publisher's note

References

Atkin, O. K., Bruhn, D., Hurry, V. M., and Tjoelker, M. G. (2005). Evans Review No. 2 - The hot and the cold: Unravelling the variable response of plant respiration to temperature. *Funct. Plant Biol.* 32, 87–105. doi: 10.1071/FP03176

Badger, M. R., Sharkey, T. D., and von Caemmerer, S. (1984). The relationship between steady-state gas exchange of bean leaves and the levels of carbon-reduction-cycle intermediates. *Planta* 160, 305–313. doi: 10.1007/BF00393411

Bernacchi, C. J., Singsaas, E. L., Pimentel, C., Portis, A. R., and Long, S. P. (2001). Improved temperature response functions for models of Rubisco-limited photosynthesis. *Plant Cell Environ.* 24, 253–259. doi: 10.1111/J.1365-3040.2001.00668.X

Borrell, A. N., Shi, Y., Gan, Y., Bainard, L. D., Germida, J. J., and Hamel, C. (2017). Fungal diversity associated with pulses and its influence on the subsequent wheat crop in the Canadian prairies. *Plant Soil* 414, 13–31. doi: 10.1007/s11104-016-3075-y

Brooks, A., and Farquhar, G. D. (1985). Effect of temperature on the CO_2/O_2 specificity of ribulose-1,5-bisphosphate carboxylase/oxygenase and the rate of respiration in the light. *Planta* 165, 397–406. doi: 10.1007/BF00392238

Busch, F. A., and Sage, R. F. (2017). The sensitivity of photosynthesis to O_2 and CO_2 concentration identifies strong Rubisco control above the thermal optimum. *New Phytol.* 213, 1036–1051. doi: 10.1111/nph.14258

Busch, F. A., Sage, T. L., Cousins, A. B., and Sage, R. F. (2013). C_3 plants enhance rates of photosynthesis by reassimilating photorespired and respired CO_2. *Plant Cell Environ.* 36, 200–212. doi: 10.1111/j.1365-3040.2012.02567.x

Caemmerer, S., and Edmondson, D. (1986). Relationship Between Steady-State Gas Exchange, *in vivo* Ribulose Bisphosphate Carboxylase Activity and Some Carbon Reduction Cycle Intermediates in Raphanus sativus. *Funct. Plant Biol.* 13, 669–688. doi: 10.1071/pp9860669

Carvalho, J. de F.C., Madgwic, P. J., and Powers, S. J. (2011). An engineered pathway for glyoxylate metabolism in tobacco plants aimed to avoid the release of ammonia in photorespiration. *BMC Biotech.* 11, 111~127. doi: 10.1186/1472-6750-11-111

Celebi-Ergin, B. (2022). Photorespiration in eelgrass (Zostera marina L.): A photoprotection mechanism for survival in a CO_2-limited world. *Front. Plant Sci.* 13. doi: 10.3389/fpls.2022.1025416

Easterling, D. R., Evans, J. L., Groisman, P. Y., Karl, T. R., Kunkel, K. E., and Ambenje, P. (2000). Observed variability and trends in extreme climate events: A brief review. *Bull. Am. Meteorol. Soc* 81, 417–425. doi: 10.1175/1520-0477(2000)081<0417:OVATIE>2.3.CO;2

Erdei, L., Horváth, F., Tari, I., Pécsváradi, A., Szegletes, Z., and Dulai, S. (2001). Differences in photorespiration, glutamine synthetase and polyamines between fragmented and closed stands of Phragmites australis. *Aquat. Bot.* 69, 165–176. doi: 10.1016/S0304-3770(01)00136-X

Ethier, G. J., and Livingston, N. J. (2004). On the need to incorporate sensitivity to CO_2 transfer conductance into the Farquhar-von Caemmerer-Berry leaf photosynthesis model. *Plant Cell Environ.* 27, 137–153. doi: 10.1111/j.1365-3040.2004.01140.x

Gan, Y., Hamel, C., O'Donovan, J. T., Cutforth, H., Zentner, R. P., Campbell, C. A., et al. (2015). Diversifying crop rotations with pulses enhances system productivity. *Sci. Rep.* 5, 14625. doi: 10.1038/srep14625

Harley, P. C., Thomas, R. B., Reynolds, J. F., and Strain, B. R. (1992). Modelling photosynthesis of cotton grown in elevated CO_2. *Plant Cell Environ.* 15, 271–282. doi: 10.1111/j.1365-3040.1992.tb00974.x

Haupt-Herting, S., Klug, K., and Fock, H. P. A. (2001). New approach to measure gross CO_2 fluxes in leaves. Gross CO_2 assimilation, photorespiration, and mitochondrial respiration in the light in tomato under drought stress. *Plant Physiol.* 126, 388–396. doi: 10.1104/pp.126.1.388

Häusler, R. E., Hirsch, H. J., Kreuzaler, F., and Peterhänsel, C. (2002). Overexpression of C_4-cycle enzymes in transgenic C_3 plants: A biotechnological approach to improve C_3-photosynthesis. *J. Exp. Bot.* 53, 591–607. doi: 10.1093/jexbot/53.369.591

Hou, R., Ouyang, Z., Li, Y., Tyler, D. D., Li, F., and Wilson, G. V. (2012). Effects of tillage and residue management on soil organic carbon and total nitrogen in the North China plain. *Soil Sci. Soc Am. J.* 76, 230–240. doi: 10.2136/sssaj2011.0107

Huang, D., Jing, G., and Zhu, S. (2023). Regulation of mitochondrial respiration by hydrogen sulfide. *Antioxidants* 12, 1644. doi: 10.3390/antiox12081644

IPCC (2021). "Climate change 2021: the physical science basis," in *Contribution of Working Group I to the Sixth Assessment Report of the Intergovernmental Panel on Climate Change* (Cambridge University Press, Oxford, UK), 7–125.

Jalali, A., Linke, M., Geyer, M., and Mahajan, P. V. (2020). Shelf life prediction model for strawberry based on respiration and transpiration processes. *Food Packag. Shelf Life* 25, 2020. doi: 10.1016/j.fpsl.2020.100525

Kang, H., Li, H., Tao, Y., and Ouyang, Z. (2014). Photosynthetic refixing of CO_2 is responsible for the apparent disparity between mitochondrial respiration in the light and in the dark (in chinese). *Acta Physiol. Plant* 36, 3157–3162. doi: 10.3724/SP.J.1258.2014.00130

Kang, H., Tao, Y., Quan, W., Wang, W., Yang, X., and Ouyang, Z. (2013). The response of photorespiration of C_3 plant to different light intensities and CO_2 concentrations (in chinese). *J. Triticeae Crops* 33, 1252–1257. doi: 10.7606/j.issn.1009-1041.2013.06.023

Krmer, K., Brock, J., and Heyer, A. (2022). Interaction of nitrate assimilation and photorespiration at elevated CO_2. *Front. Plant Sci.* 13. doi: 10.3389/fpls.2022.897924

Laisk, A., Oja, V., Rasulov, B., Rämma, H., Eichelmann, H., Kasparova, I., et al. (2002). A computer-operated routine of gas exchange and optical measurements to diagnose photosynthetic apparatus in leaves. *Plant Cell Environ.* 25, 923–943. doi: 10.1046/j.1365-3040.2002.00873.x

Lin, W. H. (1998). Response of photosynthesis to elevated atmospheric CO_2 (in chinese). *Acta Ecol. Sinica* 18, 529–538. doi: 10.3321/j.issn:1000-0933.1998.05.013

Liu, C. M., and Yu, H. N. (1997). *The Soil-Plant-Atmosphere System Experimental Study on Moisture Movement* (Beijing: Meteorological Press).

Long, S. P., and Bernacchi, C. J. (2003). Gas exchange measurements, what can they tell us about the underlying limitations to photosynthesis? Procedures and sources of error. *J. Exp. Bot.* 54, 2393–2401. doi: 10.1093/jxb/erg262

Loreto, F., Delfine, S., and Di Marco, G. (1999). Estimation of photorespiratory carbon dioxide recycling during photosynthesis. *Aust. J. Plant Physiol.* 26, 733–736. doi: 10.1071/pp99096

Loreto, F., Velikova, V., and Di Marco, G. (2001). Respiration in the light measured by $^{12}CO_2$ emission in $^{13}CO_2$ atmosphere in maize leaves. *Aust. J. Plant Physiol.* 28, 1103–1108. doi: 10.1071/pp01091

Luo, Y., Wan, S., Hui, D., and Wallace, L. L. (2001). Acclimatization of soil respiration to warming in a tall grass prairie. *Nature* 413, 622–625. doi: 10.1038/35098065

Moseley, R. C., Mewalal, R., Motta, F., Tuskan, G. A., Haase, S., and Yang, X. (2018). Conservation and diversification of circadian rhythmicity between a model crassulacean acid metabolism plant kalanchoë fedtschenkoi and a model C_3 photosynthesis plant arabidopsis thaliana. *Front. Plant Sci.* 871. doi: 10.3389/fpls.2018.01757

Nilsen, E. T. (1995). Stem photosynthesis: extent, patterns, and role in plant carbon economy. *Plant Stems*, 223–240. doi: 10.1016/B978-012276460-8/50012-6

Ostle, N., Ineson, P., Benham, D., and Sleep, D. (2000). Carbon assimilation and turnover in grassland vegetation using an in *situ* $^{13}CO_2$ pulse labelling system. *Rapid Commun. Mass Spectrom.* 14, 1345–1350. doi: 10.1002/1097-0231(20000815)14:15<1345::AID-RCM22>3.0.CO;2-B

Pärnik, T., and Keerberg, O. (2007). Advanced radiogasometric method for the determination of the rates of photorespiratory and respiratory decarboxylations of primary and stored photosynthates under steady-state photosynthesis. *Physiol. Plant.* 129, 34–44. doi: 10.1111/j.1399-3054.2006.00824.x

Parys, E., Romanowska, E., and Siedlecka, M. (2004). Light-enhanced dark respiration in leaves and mesophyll protoplasts of pea in relation to photorespiration, respiration and some metabolites content. *Acta Physiol. Plant* 26, 37–46. doi: 10.1007/s11738-004-0042-7

Pinelli, P., and Loreto, F. (2003). $^{12}CO_2$ emission from different metabolic pathways measured in illuminated and darkened C_3 and C_4 leaves at low, atmospheric and elevated CO_2 concentration. *J. Exp. Bot.* 54, 1761–1769. doi: 10.1093/jxb/erg187

Reuveni, J., and Gale, J. (1985). The effect of high levels of carbon dioxide on dark respiration and growth of plants. *Plant Cell Environ.* 8, 623–638. doi: 10.1111/j.1365-3040.1985.tb01701.x

Schimel, D. S., House, J. I., Hibbard, K. A., Bousquet, P., Ciais, P., Peylin, P., et al. (2001). Recent patterns and mechanisms of carbon exchange by terrestrial ecosystems. *Nature* 414, 169–172. doi: 10.1038/35102500

Sharkey, T. D. (1988). Estimating the rate of photorespiration in leaves. *Physiol. Plant* 73, 147–152. doi: 10.1111/j.1399-3054.1988.tb09205.x

Stirbet, A., Lazár, D., Guo, Y., and Govindjee, G. (2020). Photosynthesis: Basics, history and modelling. *Ann. Bot.* 126, 511–537. doi: 10.1093/aob/mcz171

Vaughan, D. G., Marshall, G. J., Connolley, W. M., Parkinson, C., Mulvaney, R., Hodgson, D. A., et al. (2003). Recent rapid regional climate warming on the Antarctic Peninsula. *Clim. Change* 60, 243–274. doi: 10.1023/A:1026021217991

Vercellino, I., and Sazanov, L. A. (2022). The assembly, regulation and function of the mitochondrial respiratory chain. *Nat. Rev. Mol. Cell Biol.* 23, 141–161. doi: 10.1038/s41580-021-00415-0

von Caemmerer, S. (2000). *Biochemical models of leaf photosynthesis.* (CSIRO Publishing, Collingwoo). 38. doi: 10.5860/choice.38-0936

von Caemmerer, S., and Farquhar, G. D. (1981). Some relationships between the biochemistry of photosynthesis and the gas exchange of leaves. *Planta* 153, 376–387. doi: 10.1007/BF00384257

Wang, F., Gao, J., Yong, J. W. H., Wang, Q., Ma, J., and He, X. (2020). Higher atmospheric CO_2 levels favor C_3 plants over C_4 plants in utilizing ammonium as a nitrogen source. *Front. Plant Sci.* 11. doi: 10.3389/fpls.2020.537443

Wang, X., Lewis, J. D., Tissue, D. T., Seemann, J. R., and Griffin, K. L. (2001). Effects of elevated atmospheric CO_2 concentration on leaf dark respiration of Xanthium strumarium in light and in darkness. *Proc. Natl. Acad. Sci. U. S. A.* 98, 2479–2484. doi: 10.1073/pnas.051622998

Wang, J., Yu, G., Fang, Q., Jiang, D., Qi, H., and Wang, Q. (2008). Responses of water use efficiency of nine plant species to light and CO_2 and its modeling (in chinese). *Acta Ecol. Sinica* 28, 525–533. doi: 10.3321/j.issn:1000-0933.2008.02.010

Xanthopoulos, G. T., Templalexis, C. G., Aleiferis, N. P., and Lentzou, D. I. (2017). The contribution of transpiration and respiration in water loss of perishable agricultural products: The case of pears. *Biosyst. Eng.* 158, 76–85. doi: 10.1016/j.biosystemseng.2017.03.011

Yadav, S., Rathore, M. S., and Mishra, A. (2020). The pyruvate-phosphate dikinase (C_4-SmPPDK) gene from Suaeda monoica enhances photosynthesis, carbon assimilation, and abiotic stress tolerance in a C_3 plant under elevated CO_2 conditions. *Front. Plant Sci.* 11. doi: 10.3389/fpls.2020.00345

Ye, Z. (2010). A review on modeling of responses of photosynthesis to light and CO_2 (in chinese). *Chin. J. Plant Ecol.* 34, 727–740. doi: 10.3773/j.issn.1005-264x.2010.06.012

Ye, Z., and Yu, Q. (2009). A comparison of response curves of winter wheat photosynthesis to flag leaf intercellular and air CO_2 concentrations (in chinese). *Chin. J. Ecol.* 28, 2233–2238.

Yin, X., Sun, Z., Struik, P. C., and Gu, J. (2011). Evaluating a new method to estimate the rate of leaf respiration in the light by analysis of combined gas exchange and chlorophyll fluorescence measurements. *J. Exp. Bot.* 62, 3489–3499. doi: 10.1093/jxb/err038

Zelitch, I. (1980). Measurement of photorespiratory activity and the effect of inhibitors. *Methods Enzymol.* 69, 453–464. doi: 10.1016/S0076-6879(80)69044-2

Zhang, X., Xu, D., Zhao, M., and Chen, Z. (2000). The responses of 17-years-old Chinese fir shoots to elevated CO_2 (in chinese). *Acta Ecol. Sinica* 20, 390–396.